11-3-2018

Anomalous effects of Sc substitution and processing on magnetism and structure of (Gd1−xScx)5Ge4

Jun Liu
Iowa State University and Ames Laboratory, junliu@iastate.edu

Yaroslav Mudryk
Ames Laboratory, slavkomk@ameslab.gov

Volodymyr Smetana
Iowa State University and Ames Laboratory

Anja-Verena Mudring
Iowa State University and Ames Laboratory

Vitalij K. Pecharsky
Iowa State University and Ames Laboratory, vitkp@ameslab.gov

Anomalous effects of Sc substitution and processing on magnetism and structure of (Gd1−xScx)5Ge4

Abstract
The kinetic arrest observed in the parent Gd5Ge4 gradually vanishes when a small fraction (x = 0.025, 0.05 and 0.10) of Gd is replaced by Sc in (Gd1−xScx)5Ge4, and the magnetic ground state changes from antiferromagnetic (AFM) to ferromagnetic (FM). A first order phase transition coupled with the FM-AFM transition occurs at TC = 41 K for x = 0.05 and at TC = 53 K for x = 0.10 during heating in applied magnetic field of 1 kOe, and the thermal hysteresis is near 10 K. The first-order magnetic transition is coupled with the structural Sm5Ge4-type to Gd5Si4-type transformation. The magnetization measured as a function of applied magnetic field shows sharp metamagnetic-like behavior. At the same time, the AFM to paramagnetic transition in (Gd1−xScx)5Ge4 with x = 0.10, is uncharacteristically broad indicating development of strong short-range AFM correlations above the Néel temperature. Comparison of the magnetization data of bulk, powdered, and metal-varnish composite samples of (Gd0.95Sc0.05)5Ge4 shows that mechanical grinding and fabrication of a composite have little effect on the temperature of the first-order transformation, but short-range ordering and AFM/FM ratio below TC are surprisingly strongly affected.

Disciplines
Materials Chemistry | Materials Science and Engineering

Anomalous effects of Sc substitution and processing on magnetism and structure of $(Gd_{1-x}Sc_x)_5Ge_4$

J. Liu,[1,2#] Y. Mudryk,[1*] V. Smetana,[1,3,4] A.-V. Mudring,[1,2,4] V. K. Pecharsky[1,2]

[1]*The Ames Laboratory, U.S. Department of Energy, Iowa State University, Ames, IA 50011-3020, U.S.A.*

[2]*Department of Material Science and Engineering, Iowa State University, Ames, IA 50011-2300, U.S.A.*

[3]*Department of Chemistry, Iowa State University, Ames, IA 50011-3111, U.S.A.*

[4] *Department of Materials and Environmental Chemistry, Stockholm University, Svante Arrhenius väg 16c, 10691 Stockholm, Sweden*

[#]Current Affiliation: Seagate Technology, Bloomington, MN, USA

*Corresponding author: slavkomk@ameslab.gov

Abstract

The kinetic arrest observed in the parent Gd_5Ge_4 gradually vanishes when a small fraction (x = 0.025, 0.05 and 0.10) of Gd is replaced by Sc in $(Gd_{1-x}Sc_x)_5Ge_4$, and the magnetic ground state changes from antiferromagnetic (AFM) to ferromagnetic (FM). A first order phase transition coupled with the FM-AFM transition occurs at T_C = 41 K for x = 0.05 and at T_C = 53 K for x = 0.10 during heating in applied magnetic field of 1 kOe, and the thermal hysteresis is near 10 K. The first-order magnetic transition is coupled with the structural Sm_5Ge_4-type to Gd_5Si_4-type transformation. The magnetization measured as a function of applied magnetic field shows sharp metamagnetic-like behavior. At the same time, the AFM to paramagnetic transition in $(Gd_{1-x}Sc_x)_5Ge_4$ with x = 0.10, is uncharacteristically broad indicating development of strong short-range AFM correlations above the Néel temperature. Comparison of the magnetization data of bulk, powdered, and metal-varnish composite samples of $(Gd_{0.95}Sc_{0.05})_5Ge_4$ shows that mechanical grinding and fabrication of a composite have little effect on the temperature of the first-order transformation, but short-range ordering and AFM/FM ratio below T_C are surprisingly strongly affected.

I. INTRODUCTION

Magnetostructural transformations (MSTs), which are the hallmark of the R_5T_4 family of intermetallic compounds, where R = rare earth and T = group 13-15 elements, attract strong interest since the discovery of the giant magnetocaloric effect (GMCE) in $Gd_5Si_2Ge_2$.[1] Here, and in a number of other materials, GMCE is the result of first order phase transformations where (dis/re)ordering in magnetic sublattices is coupled with major rearrangements of crystallographic sublattices. In addition to GMCE, many of R_5T_4 compounds reveal an array of interesting physical phenomena such as giant magnetostriction,[2,3] giant magnetoresistance,[4,5,6] spontaneous generation of voltage,[7,8] acoustic emissions,[9] kinetic arrest,[10,11,12] and magnetic deflagration.[13] All of these effects are rooted in strong magnetoelastic coupling, and the resulting MSTs can be controlled by external thermodynamic parameters such as temperature, hydrostatic pressure or uniaxial stress, and applied magnetic field, in addition to tuning electronic structures via chemical substitution.[14,15,16]

Gd_5Ge_4, one of most studied compounds in the R_5T_4 family, exhibits an isothermal magnetic field-induced MST between the Sm_5Ge_4-type orthorhombic (O-II) and the Gd_5Si_4-type orthorhombic (O-I) structures below 30 K. The transition is irreversible at ~9 K and below, partially reversible between 9 and ~21 K, and fully reversible above 21 K.[17,18] Further, the equivalent transition can be temperature-induced in constant applied dc magnetic fields starting at 10-14 kOe (depending on the sample), and it remains incomplete and partially irreversible[19,20] in magnetic fields lower than 30 kOe. Formation of glass-like kinetically-arrest state(s) is responsible for the irreversibility of the AFM O-II ↔ FM O-I

transition in Gd_5Ge_4 and, in addition to temperature and magnetic field, these frozen states can be controlled by hydrostatic pressure.[21] Further, this coupled MST can be made fully reversible by minor changes of the composition of the parent compound Gd_5Ge_4, for example, by substituting Ge with Si,[22,23] drastically changing magnetic properties of the system. On the other hand, substitution of Gd in Gd_5Ge_4 by as little as 5 at.% of Lu or Y can strongly suppress ferromagnetism and arrest the magnetostructural transition.[24,25]

Recently, we demonstrated that replacing Gd with non-magnetic Sc in $(Gd_{1-x}Sc_x)_5Ge_4$ both unexpectedly enhances ferromagnetism and improves reversibility of this distinctly first-order MST.[26] The key to this behavior is the unique role $3d^1$ electrons of Sc play in mediating exchange interactions between the gadolinium atoms from the neighboring slabs by hybridizing with and, consequently, enhancing magnetism of the 5*d* states of Gd, which are critically important for the magnetic exchange in rare earth compounds. In agreement with density functional theory predictions, Gd substitutions with more than 20 at.% Sc lead to a closely related Pu_5Rh_4-type structure where the first-order MST is replaced by a second-order FM ordering transition from the paramagnetic (PM) Pu_5Rh_4-type to the FM O(I)-type state, and Curie temperature, T_C, begins to decrease with increasing x due to conventional dilution effects.[26] It is worth noting that a related Gd_5Rh_4 compound, which adopts the Pu_5Rh_4-type structure, also orders magnetically via a second-order phase transformation.[27] A similar effect due to Sc substitution was observed in the $(Gd_{1-x}Sc_x)_5Si_{1.8}Ge_{2.2}$ series, although the enhancement of ferromagnetism occurs over a much narrower range of x, up to only 0.02.[28]

Clearly, replacing Gd with Sc is a capable tool for fine-tuning magnetic and structural behaviors in this and, likely, other R_5T_4 systems. With this in mind, we are presenting a detailed experimental investigation of the $(Gd_{1-x}Sc_x)_5Ge_4$ system for x = 0.025, 0.05, and 0.10 focusing on the abrupt changes in magnetic and crystal structures and unusual sensitivity of these compounds to external stimuli. We also examine how properties of a compound with x = 0.05 change upon conversion from bulk to powder and, further, to a metal-varnish composite.

II. EXPERIMENTAL PROCEDURES

A series of $(Gd_{1-x}Sc_x)_5Ge_4$ compounds with x = 0.025, 0.05 and 0.10 was prepared by arc melting of the pure elements taken in stoichiometric proportions on a water-cooled copper hearth in a Zr-gettered argon atmosphere. Elemental Gd and Sc were provided by the Materials Preparation Center of the Ames Laboratory,[29] and were at least 99.8+ at.% pure with respect to all other elements in the periodic table; Ge was 99.999+ wt.% pure, purchased from Alfa Aeser Inc. To achieve chemical homogeneities, the 5 g samples were re-melted six times, flipping them over after each melting. Phase analyses and room temperature crystal structure determinations were performed using Philips X'Pert Pro X-ray powder diffractometer employing Cu Kα_1 radiation. The powder X-ray diffraction patterns (XRD) of as cast samples indicated that they are single-phase materials with narrow Bragg peaks. All samples showed sharp transitions during physical property measurements. Further, the XRD pattern of the $Gd_{4.75}Sc_{0.25}Ge_4$ sample heat treated at 1000 °C for 3 days shows emergence of an impurity phase (not a rare earth oxide). All samples

were examined as-cast, because annealing leads to a partial decomposition of the main phase. The refinements of the measured powder XRD patterns were carried out using the Rietveld method, and the obtained lattice parameters are listed in Table 1.

Single crystal X-ray investigation was also performed for the $(Gd_{0.95}Sc_{0.05})_5Ge_4$ sample on a Bruker APEX CCD single crystal diffractometer with graphite-monochromatized Mo Kα (λ = 0.71069 Å) radiation. The raw frame data were collected at room temperature using Bruker APEX2.[30] The frames were integrated with Bruker SAINT[31] using a narrow-frame algorithm. Absorption correction was performed using the multi-scan method (SADABS).[32] All atomic positions were refined in anisotropic approximation for thermal displacements. Initial model of the crystal structure was first obtained with SHELXT-2014[33] and then refined using SHELXL[34] within Bruker APEX3. Refinement details and structural parameters are listed in Tables 2 and 3, respectively.

The magnetic properties were measured by using a superconducting quantum interference device (SQUID) magnetometer MPMS XL-7 (Quantum Design, USA). The isothermal magnetization curves were measured in magnetic fields up to 70 kOe with a 2 kOe step. Every isothermal M(H) measurements was recorded after thermal demagnetization at 200 K followed by zero field cooling down to the measurement temperature. The temperature dependence of magnetization was measured in selected dc magnetic fields using zero-field cooled (measurement on warming after cooling in zero field, ZFC) and field-cooling (measurement during cooling in field, FC) protocols. All measurements were performed on bulk polycrystalline samples unless specifically stated otherwise.

The temperature-dependent and magnetic field-dependent powder X-ray diffraction measurements were performed on a $(Gd_{0.95}Sc_{0.05})_5Ge_4$ composite (the alloy powdered and screened to particle size < 38 μm, then mixed with GE 7031 varnish and dry-solidified) from 6.3 to 300 K in magnetic fields between 0 and 30 kOe on a Rigaku TTRAX rotating anode powder diffractometer employing Mo Kα radiation. Further details about the experimental setup and sample preparation for these measurements can be found in Ref. 35.

To analyze the influence of the composite fabrication process on the material's magnetic properties we compared magnetic behaviors of bulk, powdered, and composite $(Gd_{0.95}Sc_{0.05})_5Ge_4$ samples, which were prepared as follows:

- The powdered sample was prepared by hand-grinding a piece of bulk $(Gd_{0.95}Sc_{0.05})_5Ge_4$ in an agate mortar with a pestle, followed by screening out particles greater than 38 μm. The powder was divided into four parts, one being used as is for magnetic measurements (henceforth the "powder sample").

- "Composite #1" was prepared for X-ray measurements in a copper sample holder as described in Ref. 35 using the second part of the powder sample. After the X-ray measurements were completed, a small part of the composite was chipped away and used for magnetic measurements.

- Another part of the remaining powder was mixed with GE varnish outside the Cu holder and dried to form "composite #2". While this sample was prepared using nearly identical procedure as the "composite #1", composite #2 was not restrained by the shape of a sample holder during the solidification, and, unlike "composite #1", it was not exposed to multiple

temperature and magnetic field cycling prior to the magnetization measurements. It is possible that the powder/varnish ratios were slightly different between the two composites.

- The remaining part of the powder was placed in a tantalum sleeve and then sealed in a quartz tube, evacuated and back-filled with ~3/4 atm of high-purity He gas. The tube was kept at 500 °C for 20 min, then slow-cooled to room-temperature to relieve possible stress from grinding, henceforth the "annealed powder." X-ray powder diffraction confirmed the O(II) Sm_5Ge_4–type structure of this sample at room temperature with no visible, within the sensitivity of the technique, oxide formation.

III. EXPERIMENTAL RESULTS

Crystal Structure

The room temperature powder X-ray diffraction patterns show that all prepared samples are single-phase materials retaining the O(II) Sm_5Ge_4-type orthorhombic crystal structure of the parent compound. The unit cell volume decreases as the amount of Sc substitution increases due to the smaller effective radius of the Sc atom compared to the Gd atom, as shown in Table 1. It is interesting to note that the cell contraction is anisotropic. When x(Sc) increases from 0 to 0.1 the lattice parameter a decreases by $\Delta a/a$ = -0.92 %, whilst the relative changes along the other directions are smaller: $\Delta b/b$ = -0.66 %, and $\Delta c/c$ = -0.61 %. As detailed in Ref. 26, contraction becomes more anisotropic at higher x(Sc). The crystallographic parameters of $(Gd_{0.95}Sc_{0.05})_5Ge_4$ determined by single crystal X-ray diffraction are shown in Table 3 and the refinement details are listed in Table 2. The Sc

atoms show clear preference for the 4*c* Gd1 positions (~17 %) but they are also present on the 8*d* Gd3 site (~3 %), similar to what has been found in case of Lu and Y substitutions.[24,25]

Magnetic properties

$(Gd_{0.975}Sc_{0.025})_5Ge_4$

Despite clear crystallographic similarities between the Y- and Sc-substituted Gd_5Ge_4 highlighted above, their magnetism is distinctly different. Figure 1b shows the temperature dependent magnetization of $(Gd_{0.975}Sc_{0.025})_5Ge_4$ measured between 2 and 300 K in 1 kOe applied field using ZFC heating and FC protocols (the same data for undoped Gd_5Ge_4 are shown for comparison in figure 1a). The ZFC heating curve shows a step-like decrease of the magnetization at 34 K, and a broad anomaly centered at 116 K, which signifies the AFM → PM (paramagnetic) transition occurring at Néel temperature, T_N, some 14 K lower compared to the Gd_5Ge_4 parent. The AFM↔PM transition is anhysteretic and T_N does not change during the FC measurement. On the contrary, the step-like increase of magnetization occurs at T_C = 20 K upon cooling. This low-temperature FM-like transition is not observed in the Gd_5Ge_4 parent in such a low magnetic field[17] and in $(Gd_{0.975}Sc_{0.025})_5Ge_4$ it does not fully develop due to a kinetic arrest known to occur in the parent Gd_5Ge_4, also occasionally referred to as the "magnetic glass state" due to simultaneous presence of competing AFM and FM phases.[10,11,12] The low value of magnetization is indicative of the dominant AFM O-II state, as the first-order MST transition from the AFM O-II to FM O-I state characterized by ~10,000 ppm volume change[18,19] remains kinetically arrested in low magnetic fields at low temperatures.[10]

Figure 2a shows the ZFC and FC M(T) data measured in magnetic fields of 10 and 20 kOe. The ZFC curve at 10 kOe shows a broad, plateau-like anomaly centered at ~25 K, which is similar to the M(T) behavior of Gd_5Ge_4 observed in a 16 kOe magnetic field[36] and signifies the thermal removal of the kinetic arrest when the arrested (at 2 K) ZFC sample is heated from ~2 to 20 K. The conventional first order FM O-I ↔ AFM O-II transition occurs at 35 K during heating (the temperature of AFM O-II ↔ FM O-I transition is 26 K during cooling). In 20 kOe the entire $(Gd_{0.975}Sc_{0.025})_5Ge_4$ sample is clearly FM as the kinetic arrest is removed by a strong magnetic field when applied even around 2 K, and the magnetization shows reversible first order FM ↔ AFM transition with ~6 K thermal hysteresis (T_C = 41 K for ZFC heating and 35 K for FC protocols). The AFM ↔ PM transition occurs at ~113 K in 20 kOe.

The inverse magnetic susceptibility of $(Gd_{0.975}Sc_{0.025})_5Ge_4$ follows the Curie-Weiss law above 150 K (Fig. 2b). The Weiss temperature (θ_p) is 82 K, and the effective magnetic moment (p_{eff}) is 7.96 μ_B/Gd, practically the same as the calculated moment of the free Gd^{3+} ion ($g_J[J(J+1)]^{1/2}$ = 7.94 μ_B).

Figure 3 shows the isothermal field-dependent magnetization of $(Gd_{0.975}Sc_{0.025})_5Ge_4$ measured at 2, 10, 20 and 30 K. Each plot is obtained after cooling the sample from the paramagnetic state to the desired temperature in zero field, then the field cycled twice between 0 and 70 kOe. The isothermal plot at 2 K shows a discontinuous increase of magnetization at 22 kOe, which corresponds to the field-induced removal of the kinetic arrest, thus the metastable 'frozen' AFM state transforms into the thermodynamically stable FM state. The second magnetization path is completely different from the initial one

and it follows the first demagnetization process, indicating that the sample remains in the FM state when the field is reduced to zero at this temperature. Thus, once the kinetic arrest is removed by the application of strong enough magnetic field (i.e., 22 kOe) the $(Gd_{0.975}Sc_{0.025})_5Ge_4$ phase remains ferromagnetic for the second, and, predictably, third, fourths, etc. cycles. Comparing the *M*(H) plots measured at 10 and 20 K with the 2 K data, the critical field required to trigger kinetic de-arrest is quickly decreasing as the temperature is increasing, confirming a gradual thermal removal of the kinetic arrest.

The *M*(H) data at and above 10 K exhibit a more gradually developing transition unlike the truly discontinuous behavior at 2 K. However, the AFM → FM transition remains irreversible up to at least 20 K. At 30 K, the critical field increases (compared to 20 K data) and the AFM → FM transition becomes partially reversible as the second magnetization process also shows the metamagnetic-like transition indicating that some of the FM phase (~1/6 based on the magnetization signal ratio) transformed back into the AFM state when the magnetic field was isothermally removed. These results agree with the ZFC *M*(T) data, which show that at 20 kOe the material is FM for all temperatures below T_C but at 10 kOe it is ferromagnetic in the limited temperature range only. Overall, the behavior of the $(Gd_{0.975}Sc_{0.025})_5Ge_4$ compound (2.5 at.% Sc substitution) is similar to the parent Gd_5Ge_4 compound, even though there is a clear indication that even such a minor presence of Sc decreases the critical field of the magnetostructural AFM to FM transformation. The opposite effect was observed in $(Gd_{0.975}Lu_{0.025})_5Ge_4$ where 2.5% Lu substitution drastically increases the critical field.[37]

(Gd$_{0.95}$Sc$_{0.05}$)$_5$Ge$_4$

Temperature dependence of magnetization of $(Gd_{0.95}Sc_{0.05})_5Ge_4$ measured in 1 kOe magnetic field (Fig. 4) reveals two anomalies: the FM → AFM transition at T_C = 41 K (during heating) and the AFM → PM transition at T_N = 102 K. We note that T_N for $(Gd_{0.95}Sc_{0.05})_5Ge_4$ is substantially lower compared to that of Gd_5Ge_4; moreover, this phase transition further broadens, and can be identified unambiguously only by analyzing dM/dT (not shown). There is a strong thermal hysteresis between the ZFC and FC curves, about 12 K, associated with the O(I) FM ↔ O(II) AFM magnetostructural transition. The majority phase in this compound with x = 0.05 is ferromagnetic below T_C even in fields as low as H = 1 kOe, as confirmed by the isothermal magnetization measurements, Fig. 5. Therefore, by substituting 5 % of Gd by Sc the kinetically arrested state, present in both Gd_5Ge_4 and $(Gd_{0.975}Sc_{0.025})_5Ge_4$, is completely removed in the bulk sample. Below 30 K, the M(H) curves exhibit ferromagnetic behavior with small hysteresis and clear saturation at μ_s = 7 μ_B/Gd. At 40 K and above, a distinct magnetic field-induced first-order AFM-FM phase transition with strong hysteresis is observed. The critical field of this metamagnetic-like AFM-FM transition is increasing with temperature with a rate dH_C/dT = 2.3 kOe/K. The ZFC and FC M(T) curves measured at H > 10 kOe (Fig. 6) show that the Curie temperature increases with magnetic field at a rate of ~0.3 K/kOe, which is smaller than 0.8 K/kOe reported for Gd_5Ge_4. Interestingly, while the transition remains very sharp in high field the thermal hysteresis narrows. The Curie-Weiss fit of the 20 kOe H/M data of $(Gd_{0.95}Sc_{0.05})_5Ge_4$ sample results in θ_p = 70 K and p_{eff} = 7.87 μ_B/Gd.

(Gd$_{0.9}$Sc$_{0.1}$)$_5$Ge$_4$

The *M*(T) data of (Gd$_{0.9}$Sc$_{0.1}$)$_5$Ge$_4$ measured in 1 and 20 kOe applied field (Fig. 7a) exhibit magnetostructural transition similarly to (Gd$_{0.95}$Sc$_{0.05}$)$_5$Ge$_4$ but with higher T_C (53 K on heating). While the FM transition in this compound is actually sharper compared to the one with x = 0.05 the presence of long-range AFM order cannot be confirmed for x = 0.1 using M(T) data - the AFM-PM transition cannot be unambiguously identified although a clear deviation from the Curie-Weiss behavior is observed below ~100 K. In 20 kOe magnetic field the positive deviation from linearity in the temperature dependence of the inverse susceptibility is clearly seen and it supports the presence of AFM interactions above T_C (Fig. 7b). Earlier it was suggested that in (Gd$_{0.9}$Sc$_{0.1}$)$_5$Ge$_4$ and alloys with higher x(Sc)[26] short range magnetic correlations persist down to the transition at T_C. However, heat capacity measurements of (Gd$_{0.9}$Sc$_{0.1}$)$_5$Ge$_4$ (see inset to Figure 7a) indicate a clear anomaly at T_N = 83 K suggesting possible onset of long-range ordering at this temperature. At the same time, it has to be noted that the transition at 83 K may be electronic in nature, considering that a change in electric transport behavior was observed at T_N in Gd$_5$Ge$_4$.[38]

There is a strong thermal hysteresis (9 K) associated with the phase transition at T_C, and the transition remains sharp in 20 kOe (Fig. 7a) indicating its first order. The Curie temperature increases with applied magnetic field (dT_C/dH= ~0.4 K/kOe) similar to Gd$_5$Si$_{0.5}$Ge$_{3.5}$ where dT_C/dH= 0.43 K/kOe.[23] The Curie-Weiss fit of the 20 kOe H/M vs. T data of (Gd$_{0.9}$Sc$_{0.1}$)$_5$Ge$_4$ yields effective magnetic moment p_{eff} = 7.89 μ_B/Gd and Weiss temperature θ_p = 74 K. Isothermal *M*(H) measurements (Fig. 8) confirm that the ground state of this compound is ferromagnetic. Between 50 and 60 K, a sharp metamagnetic

phase transition accompanied by strong hysteresis is observed and the critical field of the transition increases with increasing temperature with a rate dH_{cr}/dT = ~2.5 kOe/K.

Short-Range Correlations and Griffiths phase

The presence of short range correlations has been thoroughly studied in Gd_5Ge_4.[39] Figure 9 shows the temperature dependence of the inverse dc magnetic susceptibility of all samples under study measured in 100 Oe applied field and the Curie-Weiss fits to the experimental data. Significant negative deviations from the Curie-Weiss behaviors indicate the existence of short-range correlations and possible presence of the Griffiths-like phase in all of the Sc substituted samples below a characteristic temperature T_G, which is slightly above 200 K. The Griffiths-like phase, which originates from local disorder within the crystal lattice resulting in short-range magnetic clustering, is reported to occur in many $R_5(Si_xGe_{1-x})_4$ compounds (R = Gd, Tb, Dy, and Ho), and considering the similarity in physical behavior it is reasonable to assume its occurrence in studied $(Gd_{1-x}Sc_x)_5Ge_4$ as well.[40,41] We note that T_G decreases from 228 K for x = 0.025 to 210 K for x = 0.10.

When the applied magnetic field is increased to 1 kOe, only the $(Gd_{0.9}Sc_{0.1})_5Ge_4$ sample still clearly shows the Griffiths-like phase behavior below ~140 K (not shown). Interestingly, as shown in Figure 7b, further increase of the magnetic field results in a positive deviation from the Curie-Weiss fit. Such deviation is not indicative of the Griffiths phase, whose properties include suppression by high magnetic fields and negative deviation from linearity of the Curie-Weiss fit, and, in principle, confirms presence of AFM ordering. At first glance, the enhancement of such interactions by a strong applied magnetic field may appear counterintuitive, but it is important to realize that the AFM order in

Gd_5Ge_4-based systems stems from the antiparallel alignment of FM-ordered magnetic layers (slabs).[42] Therefore, it should not come as a surprise that the increased strength of the magnetic field leads to a more collinear alignment of the moments within the slabs and, consequently, a more complete moment cancellation in this unusual AFM state.

Temperature dependent X-ray diffraction

Temperature dependent powder X-ray diffraction experiments performed in the absence of magnetic field show that $(Gd_{0.95}Sc_{0.05})_5Ge_4$ undergoes a partial crystallographic change from the O(II) to the O(I) structure at ~35 K during heating and a reverse structural transformation occurs at ~25 K during cooling. A ~10 K thermal hysteresis observed for the structural change is in good agreement with 9 K hysteresis found in the magnetization measurements. The temperature dependence of the O(I) phase concentration calculated using Rietveld refinement of the obtained powder X-ray diffraction patterns is shown in Fig. 10. Unlike for Gd_5Ge_4,[17] the structural phase transition in $(Gd_{0.95}Sc_{0.05})_5Ge_4$ can be observed without application of an external magnetic field. At the same time, this phase transformation is largely incomplete, at least in a zero magnetic field, and only about a half of the material undergoes the O(II) – O(I) transition.

Figure 11 shows the temperature dependences of lattice parameters and unit cell volume of both O(II) and O(I) $(Gd_{0.95}Sc_{0.05})_5Ge_4$ phases in zero applied field calculated using Rietveld refinement of the obtained powder X-ray diffraction patterns. Clear step-like changes of the lattice parameters and unit cell volume on cooling are observed between the two phases. Similar to the parent Gd_5Ge_4, no thermal expansion anomaly is observed around the AFM-PM transition at T_N = 102 K. The discontinuous changes of the lattice

parameters $\Delta a/a$, $\Delta b/b$, $\Delta c/c$, and unit cell volume $\Delta V/V$, associated with the O(II) → O(I) structural transition are -1.96%, +0.08%, +0.75%, and −1.14%, respectively, in agreement with the reported results for Gd_5Ge_4 ($\Delta a/a = -1.9\%$, $\Delta b/b = +0.1\%$, $\Delta c/c = +0.6\%$, $\Delta V/V = -1.2\%$).[19] The largest change of the lattice parameter *a* is caused by the shear displacements of slabs along the *a* crystallographic direction during the O(II) → O(I) structural transformation.

The presence of high-temperature phases below MST temperatures is a common phenomenon in $R_5(Si_xGe_{1-x})_4$ compounds.[43] Nevertheless, for $(Gd_{0.95}Sc_{0.05})_5Ge_4$, the ratio of the O(II) and O(I) phases at 6.3 K is almost 1:1, presenting an example of stable, long-lived phase separation. In general, there could be several reasons for the incompleteness of the temperature-induced structural phase transitions, namely the presence of the structural imperfections, such as the impurities, defects, dislocations, or stresses, and the competition between magnetic and strain energies.[19,44] It is worth noting that the samples in this study were not annealed due to appearance of an impurity phase after heat treatment (see section II), so minor inhomogeneities are expected both in the distribution of defects and stress, and in the Gd/Sc ratio. At the same time, considering that the saturation magnetization of bulk $(Gd_{0.95}Sc_{0.05})_5Ge_4$ sample reaches 7 μ_B/Gd value, one can safely suggest that the O(II) AFM – O(I) FM transition is nearly complete in a bulk sample under applied field.

To clarify the role of applied field the isothermal powder X-ray diffraction measurements were performed at 30 K varying field between 0 to 30 kOe. The application of 30 kOe magnetic field increases the O(I) phase content from 3.5 % to 76.5 mol.%, as shown in Fig. 12. The isothermal magnetization of the same $(Gd_{0.95}Sc_{0.05})_5Ge_4$ composite #1 (see section

II for materials description) used in the powder X-ray diffraction experiment was measured at 30 K and is normalized using the formula $M = M_0/M(30\,K, 30\,kOe) \times C_{O(I)}(30\,K, 30\,kOe)$, where M is the magnetization and $C_{O(I)}$ is the concentration of the O(I) phase determined from the powder X-ray diffraction experiment. The isothermal magnetization curve clearly correlates with the structural changes, confirming the intimate coupling between the magnetic and crystal lattices in $(Gd_{0.95}Sc_{0.05})_5Ge_4$.

Still, it is important to keep in mind that the structural properties reported above are those of the powdered $(Gd_{0.95}Sc_{0.05})_5Ge_4$ sample that was solidified with a GE varnish, effectively a metal-varnish composite. The differences in the behavior of bulk and powder specimens are to be expected and will be analyzed next.

Effect of composite fabrication process on the magnetic properties of $(Gd_{0.95}Sc_{0.05})_5Ge_4$

The difference in the observed magnetostructural behavior between bulk and composite (powder+GE varnish) samples, e.g. between M(H)@30 K data shown in Figures 5 and 12, may be caused by sample grinding, which introduces defects and strain. Further, stress/strain effects due to a relatively rigid matrix environment, a competition between magnetic and strain energies, mentioned above, or any combination of these factors may also play a role. The presence of additional stress imposed on a sample by a potentially inelastic GE varnish[a] was reported to be a factor in low-temperature thermal expansion studies.[45] Stress generation due to differences in thermal expansion coefficients between

[a] To the best of our knowledge no data on the thermal expansion of GE 7031 varnish, which is commonly used in cryogenic applications such as our XRD experiment, are publicly available.

the intermetallic powder and the varnish is to be expected; however, in R_5T_4 alloys the observed influence of the stress caused by GE varnish matrix on the MST was found to be insignificant. For example, the Er_5Si_4 compound is extremely sensitive to external pressure, dTs/dP = ~-30 K/kbar,[46] yet the structural transition temperature is not affected by the powder being embedded into the varnish.[47] On the other hand, prolonged room temperature mechanical grinding (although for much longer times than commonly needed for routine powder preparation for x-ray diffraction experiments) in an inert atmosphere was shown to trigger a structural transition in Er_5Si_4,[48] which is reversed after annealing.

Consequently, to study how two major sample preparation steps, i.e., grinding and solidification in a varnish, influence the magnetic behavior of $(Gd_{0.95}Sc_{0.05})_5Ge_4$, we measured and compared magnetization of powders, raw and annealed, and composite materials with that of a bulk sample (Figures 13, 14). Because for the composite materials the exact powder/varnish ratio is unknown the direct comparison of absolute values is not possible and some normalization procedure has to be applied. For example, we can assume that the magnetic susceptibility in the strictly paramagnetic region, i.e. at 300 K, should be identical for the same amount of Gd ions (the diamagnetic contribution from GE varnish is neglected), so we normalized the magnetization of the composite to match that of the powder and bulk sample at 300 K for the M(T) data collected at H = 1 kOe, i.e. $M_{norm} = M/M_{300K}$ so each sample has M = 1 at 300 K. Figure 13a compares M(T) data of bulk, powder, and composite #1 (X-ray sample), while the Figure 13b shows how the properties of the powder sample change after mixing with GE varnish or annealing. The values of M in the FM state are ambiguous due to low value of the applied magnetic field but the

observed differences between transition temperatures and/or *M* values in the paramagnetic state can be reliably analyzed.

The main change occurs after grinding, i.e., upon conversion of bulk sample into powder. The T_C of powder sample is lowered by a few K relative to bulk and the phase transformation becomes broader and more hysteretic. Furthermore, there is a substantial increase in magnetization around 150 K, which is above T_C and T_N but below T_G (a broad anomaly at T_N is still observed). This indicates a strong enhancement of short-range magnetic correlations via formation of magnetic clusters although the exact mechanism of such enhancement is not fully understood. Further processing of the powder, either mixing with varnish or annealing, does not profoundly influence the magnetostructural transition, yet short-range magnetism is enhanced in composite materials, but it is moderately suppressed in the annealed powder. In the composites, especially in composite #2, the Griffiths-phase behavior remains prominent in 1 kOe and the increase in *M*(T) coincides with T_G determined from 100 Oe data (Figure 9), while in the bulk sample, 1 kOe field practically quenches the Griffiths-like phase. The lower T_C of powders compared to bulk samples is a common phenomenon in $R_5(Si_xGe_{1-x})_4$ compounds and was observed for $Gd_5Si_{0.5}Ge_{3.5}$[23] and $Tb_5Si_{2.2}Ge_{1.8}$.[49]

The data for the isothermal *M*(H) measurement at 5 K were normalized in a different way, namely the saturated value at 70 kOe was assigned as $M = 1$, so $M = M_0/M_{7T}$. A significant difference was observed again between the powder and the bulk sample, while the difference between the power and the X-ray composite #1 is miniscule (Figure 14). Unlike bulk sample, which is almost fully ferromagnetic at 5 K, the powder and the composite

exhibit a modest increase of magnetization with applied field below ~12 kOe followed by a field-induced step-like transition at $H_{cr} \cong 14$ kOe. The initial increase in magnetization reflects the presence of the FM O(I) phase, while the step-like increase is due to the metamagnetic-like transformation of the remaining AFM O(II) phase. The ratio between the saturation magnetization before and after the magnetic-field-induced transformation shows that both the zero field cooled powder sample and composite #1 contain nearly equal amounts of FM and AFM phases, in full agreement with the powder X-ray diffraction experiment, where incomplete (~50%) O(II) to O(I) structural transformation was observed (Figure 10). During the second magnetization and demagnetization cycles (not shown), the M(H) curve follows the first demagnetization path, indicating that the majority of the sample remains in the FM state and the metamagnetic transition observed in the virgin material is irreversible.

These findings show a remarkable effect that short (a minute or so) room temperature mechanical grinding has on the low-temperature magnetostructural properties of $(Gd_{0.95}Sc_{0.05})_5Ge_4$: while the bulk sample is fully ferromagnetic below T_C, the powder retains a significant amount of the AFM O(II) phase. The application of magnetic field above 14 kOe at T = 5 K completely removes the mechanically induced metastability negating the effects of mechanical grinding and creating a homogeneous ferromagnetic system. Annealing the powder can further reduce the amount of FM phase in a zero-field cooled sample. The M(H) data, as displayed in Fig. 14b, suggest that there is only about 30% of O(I) phase at 5 K in the annealed powder. On one hand, this may be easily explained by the incorporation of interstitial oxygen during grinding and annealing, that can, presumably, stabilize O(II) phase. This, however, contradicts the previous body of work

on Gd_5T_4 systems, because preparing samples with less pure rare earths typically leads to the stabilization of the O(I) structure. It is worth to note that mixing the as-milled powder with the varnish (composite #2) also reduces the amount of the O(I) phase at 5 K. The notable difference in the magnetic behaviors between two composites may be related to the fact that composite #1 underwent multiple transformations prior to the measurement (training effect). This indicates that stress from the matrix is an important factor and the stress-strain relationships in R_5T_4 systems are a known factor of control over magnetostructural transformations. It appears, however, that the presence of internal stress in bulk alloys promotes the completion of magnetostructural O(II) AFM → O(I) FM transition in $(Gd_{0.95}Sc_{0.05})_5Ge_4$ material similarly to how the stress introduced by thin plates activates the metamagnetic process in $Gd_5Si_2Ge_2$ compound.[50] Another plausible explanation for the reduced amount of the O(I) phase in the powder sample compared to the bulk is the increase of the nucleation field when the particle size is reduced below a typical size of the nucleation cluster during the mechanical grinding.[51] In any case, the material can be easily trained to be FM below T_C, as shown by the cycling experiment.

IV. CONCLUSIONS

A detailed experimental study of minor Gd by Sc substitution in $(Gd_{1-x}Sc_x)_5Ge_4$ alloys for x = 0.025, 0.05, and 0.1 has been carried out. The dominant antiferromagnetic behavior with a signature of the frustrated FM interactions (kinetic arrest) was found in $(Gd_{0.975}Sc_{0.025})_5Ge_4$. At higher concentrations of Sc, $(Gd_{0.95}Sc_{0.05})_5Ge_4$ and $(Gd_{0.9}Sc_{0.1})_5Ge_4$ compounds are ferromagnetic with T_C = 41 and 53 K (on heating), respectively. Strong AFM short-range behaviors are present in $(Gd_{0.9}Sc_{0.1})_5Ge_4$ above T_N even in 20 kOe field.

The temperature dependent powder X-ray diffraction measurements confirm the presence of magnetostructural O(II) AFM → O(I) FM transition in $(Gd_{0.95}Sc_{0.05})_5Ge_4$ at T_C, however, the transition appears to be incomplete. The investigation of bulk, powdered and metal-varnish composite samples shows that the pulverization has a strong influence on magnetic behavior. The powdered samples show a significant enhancement of short-range magnetic clustering and more robust kinetic arrest. We suggest that the mechanical grinding of $(Gd_{0.95}Sc_{0.05})_5Ge_4$ increases the nucleation energy barrier for the magnetostructural O(II) AFM → O(I) FM transition in $(Gd_{0.95}Sc_{0.05})_5Ge_4$ compound resulting in only a ~50% completion in zero field. Apparently, the kinetic arrest of composite $(Gd_{0.95}Sc_{0.05})_5Ge_4$ samples can be removed by applied magnetic field or reduced by multiple cycling (training).

Acknowledgments

The Ames Laboratory is operated for the U. S. Department of Energy by Iowa State University of Science and Technology under contract No. DE-AC02-07CH11358. This work was supported by the Department of Energy, Office of Basic Energy Sciences, Materials Sciences Division.

References

[1] V. K. Pecharsky and K. A. Gschneidner, Jr., Giant magnetocaloric effect in $Gd_5(Si_2Ge_2)$, Phys. Rev. Lett. 78 (1997) 4494.

[2] L. Morellon, J. Blasco, P. A. Algarabel, and M. R. Ibarra, Nature of the first-order antiferromagnetic-ferromagnetic transition in the Ge-rich magnetocaloric compounds $Gd_5(Si_xGe_{1-x})_4$, Phys. Rev. B 62 (2000) 1022.

[3] L. Morellon, P. A. Algarabel, M. R. Ibarra, J. Blasco, B. García-Landa, Z. Arnold, and F. Albertini, Magnetic-field-induced structural phase transition in $Gd_5(Si_{1.8}Ge_{2.2})$, Phys. Rev. B 58 (1998) R14721.

[4] L. Morellon, J. Stankiewicz, P. A. Algarabel, B. García-Landa, and M. R. Ibarra, Giant magnetoresistance near the magnetostructural transition in $Gd_5(Si_{1.8}Ge_{2.2})$, Appl. Phys. Lett. 73 (1998) 3462.

[5] E. M. Levin, V. K. Pecharsky, and K. A. Gschneidner, Jr., Magnetic-field and temperature dependencies of the electrical resistance near the magnetic and crystallographic first-order phase transition of $Gd_5(Si_2Ge_2)$, Phys. Rev. B 60 (1999) 7993.

[6] E. M. Levin, V. K. Pecharsky, K. A. Gschneidner, Jr., and P. Tomlinson, Magnetic field and temperature induced first-order transition in $Gd_5(Si_{1.5}Ge_{2.5})$: A study of the electrical resistance behavior, J. Magn. Magn. Mater. 210 (2000) 181.

[7] E. M. Levin, V. K. Pecharsky, and K. A. Gschneidner Jr., Spontaneous generation of voltage in $Gd_5(Si_xGe_{4-x})$ during a first-order phase transition induced by temperature or magnetic field, Phys. Rev. B 63 (2001) 174110.

[8] M. Zou, V. K. Pecharsky, K. A. Gschneidner Jr., D. L. Schlagel, and T. A. Lograsso, Spontaneous generation of voltage in the magnetocaloric compound $Tb_5Si_{2.2}Ge_{1.8}$ and elemental Gd, J. Alloys Compd. 488 (2009) 550.

[9] F. J. Pérez-Reche, F. Casanova, E. Vives, L. Mañosa, A. Planes, J. Marcos, X. Batlle, and A. Labarta, Acoustic emission across the magnetostructural transition of the giant magnetocaloric $Gd_5Si_2Ge_2$ compound, Phys. Rev. B 73 (2006) 014110.

[10] S. B. Roy, M. K. Chattopadhyay, P. Chaddah, J. D. Moore, G. K. Perkins, L. F. Cohen, K. A. Gschneidner Jr., and V. K. Pecharsky, Evidence of a magnetic glass state in the magnetocaloric material Gd_5Ge_4, Phys. Rev. B 74 (2006) 012403.

[11] Z. Ouyang, V. K. Pecharsky, K. A. Gschneidner, Jr, D. L. Schlagel, and T. A. Lograsso, Field step size and temperature effects on the character of the magneto-structural transformation in a Gd_5Ge_4 single crystal, Phys. Rev. B 76 (2007) 134406.

[12] M.K. Chattopadhyay, S.B. Roy, K. Morrison, J.D. Moore, G.K. Perkins, L.F. Cohen, K.A. Gschneidner, Jr., V.K. Pecharsky, Visual evidence of the magnetic glass state and its re-crystallization in Gd_5Ge_4, Euro. Phys. Lett. 83 (2008) 57006.

[13] S. Velez, J. M. Hernandez, A. Fernandez, F. Macià, C. Magen, P. A. Algarabel, J. Tejada, and E. M. Chudnovsky, Magnetic deflagration in Gd_5Ge_4, Phys. Rev. B 81 (2010) 064437.

[14] Ya. Mudryk, Y. Lee, T. Vogt, K. A. Gschneidner Jr., and V. K. Pecharsky, Polymorphism of $Gd_5Si_2Ge_2$ – the equivalence of temperature, magnetic field, and chemical and hydrostatic pressures, Phys. Rev. B 71 (2005) 174104.

[15] J. Yao, Y. Zhang, P. L. Wang, L. Lutz, G. J. Miller, Yu. Mozharivskyj, Electronically induced ferromagnetic transitions in Sm_5Ge_4-type magnetoresponsive phases, Phys. Rev. Lett. 110 (2013) 077204.

[16] Y. C. Tseng, D. Paudyal, Ya. Mudryk, V. K. Pecharsky, K. A. Gschneidner, Jr., D. Haskel, Electronic contribution to the enhancement of the ferromagnetic ordering temperature by Si substitution in $Gd_5(Si_xGe_{1-x})_4$ system, Phys. Rev. B 88 (2013) 054428.

[17] H. Tang, V. K. Pecharsky, K. A. Gschneidner Jr., and A. O. Pecharsky, Interplay between reversible and irreversible magnetic phase transitions in polycrystalline Gd_5Ge_4, Phys. Rev. B 69 (2004) 064410.

[18] V.K. Pecharsky, A.P. Holm, K.A. Gschneidner Jr., and R. Rink, Massive magnetic-field-induced structural transformation in Gd_5Ge_4 and nature of the giant magnetocaloric effect, Phys. Rev. Lett. 91 (2003) 197204.

[19] Ya. Mudryk, A. P. Holm, K. A. Gschneidner Jr., and V. K. Pecharsky, Crystal structure – magnetic property relationships of Gd_5Ge_4 examined by *in situ* x-ray powder diffraction, Phys. Rev. B 72 (2005) 064442.

[20] Z. Ouyang, V.K. Pecharsky, K.A. Gschneidner, Jr, D.L. Schlagel, and T.A. Lograsso, Magnetic anisotropy and magnetic phase diagram of Gd_5Ge_4, Phys. Rev. B 74 (2006) 024401.

[21] C. Magen, Z. Arnold, L. Morellon, Y. Skorokhod, P. A. Algarabel, M. R. Ibarra, and J. Kamarad, Pressure-induced three-dimensional ferromagnetic correlations in the giant magnetocaloric compound Gd_5Ge_4, Phys. Rev. Lett. 91 (2003) 207202.

[22] Y. C. Tseng, D. Haskel, J. C. Lang, S. Sinogeikin, Ya. Mudryk, V. K. Pecharsky, and K. A. Gschneidner, Jr., The effect of hydrostatic pressure upon the magnetic transitions in the $Gd_5(Si_xGe_{1-x})_4$ giant magnetocaloric compounds: an x-ray magnetic circular dichroism study, Phys. Rev. B 76 (2007) 014411.

[23] Y. Mudryk, D. Paudyal, V. K. Pecharsky, and K. A. Gschneidner, Jr., Magnetostructural transition in $Gd_5Si_{0.5}Ge_{3.5}$: magnetic and x-ray powder diffraction measurements, and theoretical calculations, Phys. Rev. B **77** (2008) 024408.

[24] Y. Mudryk, D. Paudyal, V. K. Pecharsky, K. A. Gschneidner Jr., S. Misra and G. J. Miller, Controlling magnetism of a complex metallic system using atomic individualism, Phys. Rev. Lett. 105 (2010) 066401.

[25] D. Paudyal, Y. Mudryk, V. K. Pecharsky, S. Misra, G. J. Miller, and K. A. Gschneidner Jr., Influence of Y substitutions on the magnetism of Gd_5Ge_4, J. Appl. Phys. 107 (2010) 09A908.

[26] Y. Mudryk, D. Paudyal, J. Liu, V. K. Pecharsky, Enhancing magnetic functionality with scandium: Breaking stereotypes in the design of rare earth materials, Chem. Mater. 29 (2017) 3962.

[27] C. L. Wang, J. D. Zou, J. Liu, Y. Mudryk, K. A. Gschneidner Jr., Y. Long, V. Smetana, G. J. Miller, V. K. Pecharsky, Crystal structure, magnetic properties, and the magnetocaloric effect of Gd_5Rh_4 and GdRh, J. Appl. Phys. 113 (2013) 17A904.

[28] K. Rudolph, A. K. Pathak, Y. Mudryk, V. K. Pecharsky, Magnetostructural phase transitions and magnetocaloric effect in $(Gd_{5-x}Sc_x)Si_{1.8}Ge_{2.2}$, Acta Mater. 145 (2018) 369.

[29] Materials Preparation Center, Ames Laboratory US-DOE, Ames, IA, USA, www.mpc.ameslab.gov.

[30] APEX2/APEX3. Bruker AXS Inc., Madison, Wisconsin, USA, 2015.

[31] SAINT. Bruker AXS Inc., Madison, Wisconsin, USA, 2015.

[32] L. Krause, R. Herbst-Irmer, G. M. Sheldrick, and D. Stalke, Comparison of silver and molybdenum microfocus X-ray sources for single-crystal structure determination, J. Appl. Crystallogr. 48 (2015) 3-10.

[33] G. Sheldrick, SHELXT - Integrated space-group and crystal-structure determination, Acta Crystallogr. Sect. A 71 (2015) 3-8.

[34] G. Sheldrick, Crystal structure refinement with SHELXL, Acta Crystallogr. Sect. C: Struct. Chem. 71 (2015) 3-8.

[35] A. P. Holm, V. K. Pecharsky, K. A. Gschneidner Jr., R. Rink, and M. N. Jirmanus, A high resolution X-ray powder diffractometer for *in situ* structural studies in magnetic fields from 0 to 35 kOe between 2.2 and 315 K, Rev. Sci. Instrum.75 (2004) 1081.

[36] E. M. Levin, V. K. Pecharsky, and K. A. Gschneidner Jr., Magnetic correlations induced by magnetic field and temperature in Gd_5Ge_4, Phys. Rev. B 65 (2002) 214427.

[37] Y. Mudryk, V. K. Pecharsky, and K. A. Gschneidner, Unusual magnetic frustration in Lu-doped Gd_5Ge_4, J. Appl. Phys. 113 (2013) 17E104.

[38] E. M. Levin, V. K. Pecharsky, K. A. Gschneidner, Jr., and G. J. Miller, Electrical resistivity, electronic heat capacity, and electronic structure of Gd_5Ge_4, Phys. Rev. B 64 (2001) 235103.

[39] Z. Ouyang, V. K. Pecharsky, K. A. Gschneidner, Jr, D. L. Schlagel, and T. A. Lograsso, Short range anisotropic ferromagnetic correlations in the paramagnetic and antiferromagnetic phases of Gd_5Ge_4, Phys. Rev. B 74**,** (2006) 094404.

[40] C. Magen, P. A. Algarabel, L. Morellon, J. P. Araujo, C. Ritter, M. R. Ibarra, A. M. Pereira, and J. B. Sousa, Observation of a Griffiths phase in the magnetocaloric compound $Tb_5Si_2Ge_2$, Phys. Rev. Lett. 96 (2006) 167201.

[41] A. M. Pereira, L. Morellon, C. Magen, J. Ventura, P. A. Algarabel, M. R. Ibarra, J. B. Sousa, and J. P. Araújo, Griffiths-like phase of magnetocaloric $R_5(Si_xGe_{1-x})_4$ (R = Gd, Tb, Dy, and Ho), Phys. Rev. B 82 (2010) 172406.

[42] L. Tan, A. Kreyssig, J. W. Kim, A. I. Goldman, R. J. McQueeney, D. Wermeille, B. Sieve, T. A. Lograsso, D. L. Schlagel, S. L. Budko, V. K. Pecharsky, and K. A. Gschneidner, Jr., Magnetic structure of Gd_5Ge_4, Phys. Rev. B 71 (2005) 214408.

[43] N. K. Singh, Ya. Mudryk, V. K. Pecharsky, and K. A. Gschneidner, Jr., Magnetostructural properties of $Ho_5(Si_{0.8}Ge_{0.2})_4$, Phys. Rev. B 81 (2010) 184414.

[44] R. Nirmala, Y. Mudryk, V. K. Pecharsky, and K. A. Gschneidner Jr., Magnetic and structural transitions in Dy_5Si_3Ge, Phys. Rev. B 76 (2007) 104417.

[45] C. R. Morelock, M. R. Suchomel, and A. P. Wilkinson, A cautionary tale on the use of GE-7031 varnish: low-temperature thermal expansion studies of ScF_3, J. Appl. Crystallogr. 46 (2013) 823-825.

[46] C. Magen, L. Morellon, Z. Arnold, P. A. Algarabel, C. Ritter, M. R. Ibarra, J. Kamarad, A. O. Tsokol, K. A. Gschneidner, Jr., and V. K. Pecharsky, Effects of pressure on the magnetic and crystallographic structure of Er_5Si_4, Phys. Rev. B 74 (2006) 134427.

[47] Ya. Mudryk, N. K. Singh, V. K. Pecharsky, D. L. Schlagel, T. A. Lograsso, and K. A. Gschneidner, Jr., Magnetic and structural properties of single-crystalline Er_5Si_4, Phys. Rev. B 85 (2012) 094432.

[48] Q. Cao, L. S. Chumbley, Y. Mudryk, M. Zou, V. K. Pecharsky, K. A. Gschneidner, Jr., Effects of mechanical grinding and low temperature annealing on crystal structure of Er_5Si_4, J. Alloys Compd. 556 (2013) 127.

[49] M. Zou, Ya. Mudryk, V. K. Pecharsky, K. A. Gschneidner, Jr., D. L. Schlagel, and T. A. Lograsso, Crystallography, anisotropic magnetism and magnetocaloric effect in $Tb_5Si_{2.2}Ge_{1.8}$, Phys. Rev. B 75 (2007) 024418.

[50] J. D. Moore, K. Morrison, G. K. Perkins, D. L. Schlagel, T. A. Lograsso, K. A. Gschneidner, Jr., V. K. Pecharsky, and L. F. Cohen, Metamagnetism seeded by nanostructural features of single-crystalline $Gd_5Si_2Ge_2$, Adv. Mater. 21 (2009) 3780.

[51] J. D. Moore, G. K. Perkins, Y. Bugoslavsky, M. K. Chattopadhyay, S. B. Roy, P. Chaddah, V. K. Pecharsky, K. A. Gschneidner, Jr., and L. F. Cohen, Reducing the operational magnetic field in the prototype magnetocaloric system Gd_5Ge_4 by approaching the single cluster size limit, Appl. Phys. Lett. 88 (2006) 072501.

Figure Captions

Figure 1. (Color online) Temperature dependencies of the dc magnetization of a) Gd_5Ge_4 and b) $(Gd_{0.975}Sc_{0.025})_5Ge_4$ measured in 1 kOe applied magnetic field with ZFC and FC protocols.

Figure 2. (Color online) (a) Temperature dependencies of the dc magnetization of $(Gd_{0.975}Sc_{0.025})_5Ge_4$ measured in 10 and 20 kOe applied magnetic fields. (b) The temperature dependence of the inverse susceptibility (H/M) vs. T for 20 kOe applied field. The red solid line represents the Curie-Weiss fit to the experimental data.

Figure 3. (Color online) The isothermal magnetization of $(Gd_{0.975}Sc_{0.025})_5Ge_4$ at 2, 10, 20, and 30 K. Solid blue circles indicate the first magnetization/demagnetization cycle and the open red triangles indicate the second magnetization/demagnetization cycle.

Figure 4. (Color online) Temperature dependencies of the dc magnetization of $(Gd_{0.95}Sc_{0.05})_5Ge_4$ measured in a 1 kOe applied magnetic field with ZFC and FC protocols.

Figure 5. (Color online) The isothermal magnetization of $(Gd_{0.95}Sc_{0.05})_5Ge_4$ measured in the range of temperatures from 5 to 60 K.

Figure 6. (Color online) (a) Temperature dependencies of the dc magnetization of $(Gd_{0.95}Sc_{0.05})_5Ge_4$ measured in 10, 20, 40, and 70 kOe applied magnetic fields with ZFC and FC protocols. (b) The temperature dependence of the inverse susceptibility (H/M) vs.

T obtained under the 20 kOe applied field. The red solid line represents the Curie-Weiss fit to the experimental data.

Figure 7. (Color online) (a) Temperature dependencies of the dc magnetization of $(Gd_{0.9}Sc_{0.1})_5Ge_4$ measured in 1 kOe and 20 kOe applied magnetic field with ZFC and FC protocols. The inset highlight the AFM-PM transition observed in zero field heat capacity data between 60 and 110 K. (b) The temperature dependence of the inverse susceptibility (*H*/*M*) vs. *T* obtained under the 20 kOe applied field. The red solid line represents the Curie-Weiss fit to the experimental data.

Figure 8. (Color online) The isothermal magnetization of $(Gd_{0.9}Sc_{0.1})_5Ge_4$ measured in the range of temperatures from 2 to 90 K.

Figure 9. (Color online) The inverse dc magnetic susceptibility (*H*/*M*) of $(Gd_{1-x}Sc_x)_5Ge_4$ (x = 0.025 (a), 0.05 (b), and 0.1 (c)) measured in a 100 Oe dc magnetic field.

Figure 10. (Color online) Concentration of the O(I)-$(Gd_{0.95}Sc_{0.05})_5Ge_4$ phase as a function of temperature (symbols, left hand scale) determined from the powder X-ray diffraction experiment during heating and cooling in zero magnetic field and the dc magnetization of $(Gd_{0.95}Sc_{0.05})_5Ge_4$ powder sample measured in 1 kOe magnetic field (thick lines, right hand scale) during heating and cooling. Arbitrary units are used because the powder was mixed with varnish and its exact mass was unknown.

Figure 11. (Color online) Temperature dependencies of the lattice parameters and the unit-cell volume of $(Gd_{0.95}Sc_{0.05})_5Ge_4$ determined from 6.3 to 300 K in a zero magnetic field on cooling. The solid circles indicate lattice constants of the high-temperature O(II)

structure, which is present down to the lowest temperature of the measurement. The open circles indicate lattice constants of the high-temperature O(I) structure.

Figure 12. (Color online) The comparison of the magnetic field dependence of the O(I) phase concentration determined using the powder X-ray diffraction (open squares) with the normalized magnetization of $(Gd_{0.95}Sc_{0.05})_5Ge_4$ (solid circles) at 30 K.

Figure 13. (Color online) (a) Temperature dependency of magnetization of the $(Gd_{0.95}Sc_{0.05})_5Ge_4$ bulk, powder, and composite #1 (X-ray sample) materials measured from 2 to 300 K in magnetic field of 1 kOe. (b) Temperature dependency of magnetization of the $(Gd_{0.95}Sc_{0.05})_5Ge_4$ as-milled powder, annealed (500 °C/20 min) powder and composite #2 measured from 2 to 300 K in magnetic field of 1 kOe.

Figure 14. (Color online) (a) Isothermal dc magnetization of the bulk, powder, and composite #1 samples of $(Gd_{0.95}Sc_{0.05})_5Ge_4$ at 5 K. (b) Isothermal dc magnetization of the as-milled powder, annealed powder, and composite #2 sample of $(Gd_{0.95}Sc_{0.05})_5Ge_4$ at 5 K.

Tables

Table 1. Lattice parameters for $(Gd_{1-x}Sc_x)_5Ge_4$

x/Sc	a (Å)	b (Å)	c (Å)	V (Å^3)
0	7.6951(2)	14.8246(3)	7.7838(2)	887.95(4)
0.025	7.6764(2)	14.8023(4)	7.7691(2)	882.79(7)
0.05	7.6569(4)	14.7759(8)	7.7577(4)	877.69(13)
0.1	7.6240(3)	14.7263(5)	7.7354(3)	868.48(9)

Table 2. Crystallographic details and refinement parameters for $(Gd_{0.95}Sc_{0.05})_5Ge_4$.

Formula	$(Gd_{0.95}Sc_{0.05})_5Ge_4$
Molecular weight, g/mol	1049.43
Space group	*Pnma* (no. 62)
a, Å	7.646(1)
b, Å	14.757(3)
c, Å	7.746(1)
V [Å^3]	874.0(3)
Temperature, K	293(2)
Density (calculated), g/cm^3	7.976
Absorption coefficient, μ, mm^{-1}	49.177
F (000)	1750
θ range for data collection, °	2.761 to 28.324
Index ranges	-10 < h < 9
	-19 < k < 19
	-10 < l < 10
Intensity data collected	6788
Number of independent reflections	1095 [R_{int} = 0.1195]
Completeness, %	100
Data/ Restraints/ Parameters	1095/0/48
Goodness-of-fit (F^2)	1.071
R_1, ωR_2 [I_0>2σ (I)]	0.0312; 0.0628
R_1, ωR_2 (all data)	0.0399; 0.0656
Largest diff. peak and hole [e/Å^{-3}]	2.116 and – 1.932

Table 3. Atomic positions, equivalent isotropic thermal displacement parameters, and site occupancies of $(Gd_{0.95}Sc_{0.05})_5Ge_4$. The refined composition is $(Gd_{0.952}Sc_{0.048})_5Ge_4$.

Atom	**Wyckoff**	**x**	**y**	**z**	***U*eq**	**Occ.**
Gd1	4c	0.2928(1)	¼	0.0006(1)	0.0105(2)	0.826(4)
Sc1	4c	0.2928(1)	¼	0.0006(1)	0.0105(2)	0.174(4)
Gd2	8d	0.02152(6)	0.59956(3)	0.17862(6)	0.0114(2)	1
Gd3	8d	0.12596(6)	0.11735(3)	0.33839(6)	0.0103(2)	0.966(4)
Sc3	8d	0.12596(6)	0.11735(3)	0.33839(6)	0.0103(2)	0.034(4)
Ge1	4c	0.1763(2)	¼	0.6357(2)	0.0112(3)	1
Ge2	4c	0.4220(2)	¼	0.3868(2)	0.0118(3)	1
Ge3	8d	0.2851(1)	0.04415(7)	0.0337(1)	0.0120(2)	1

Figures

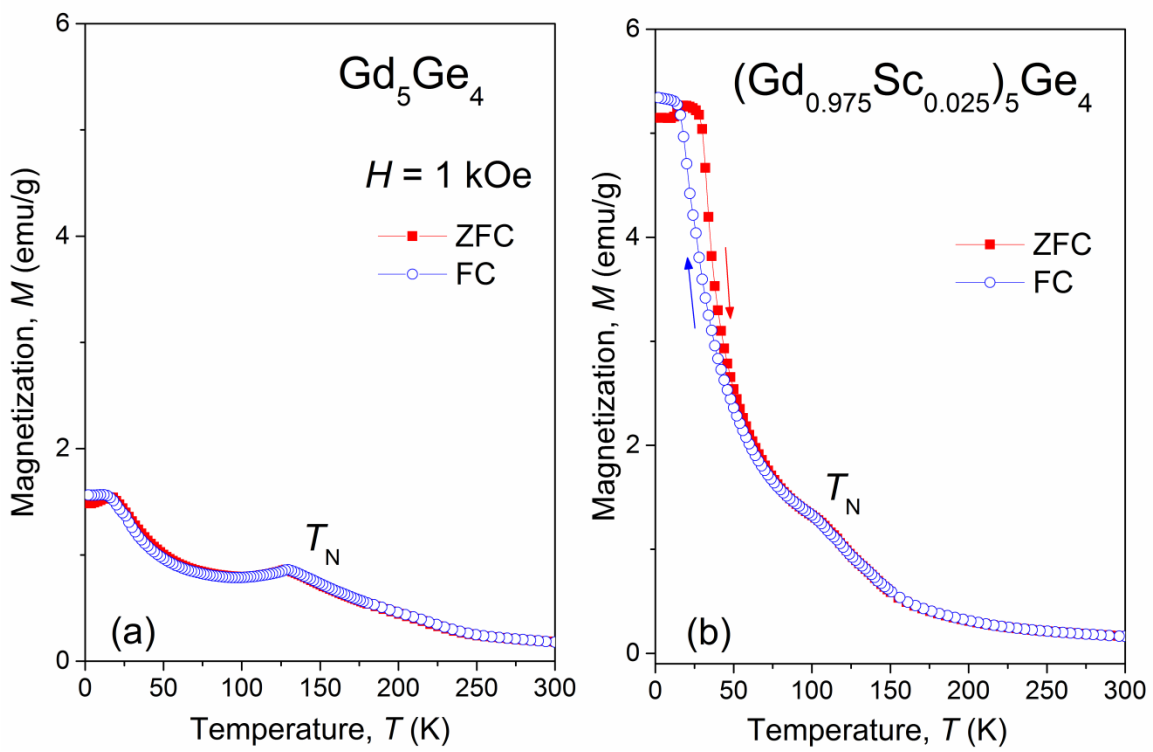

Figure 1. (Color online) Temperature dependencies of the dc magnetization of a) Gd_5Ge_4 and b) $(Gd_{0.975}Sc_{0.025})_5Ge_4$ measured in 1 kOe applied magnetic field with ZFC and FC protocols.

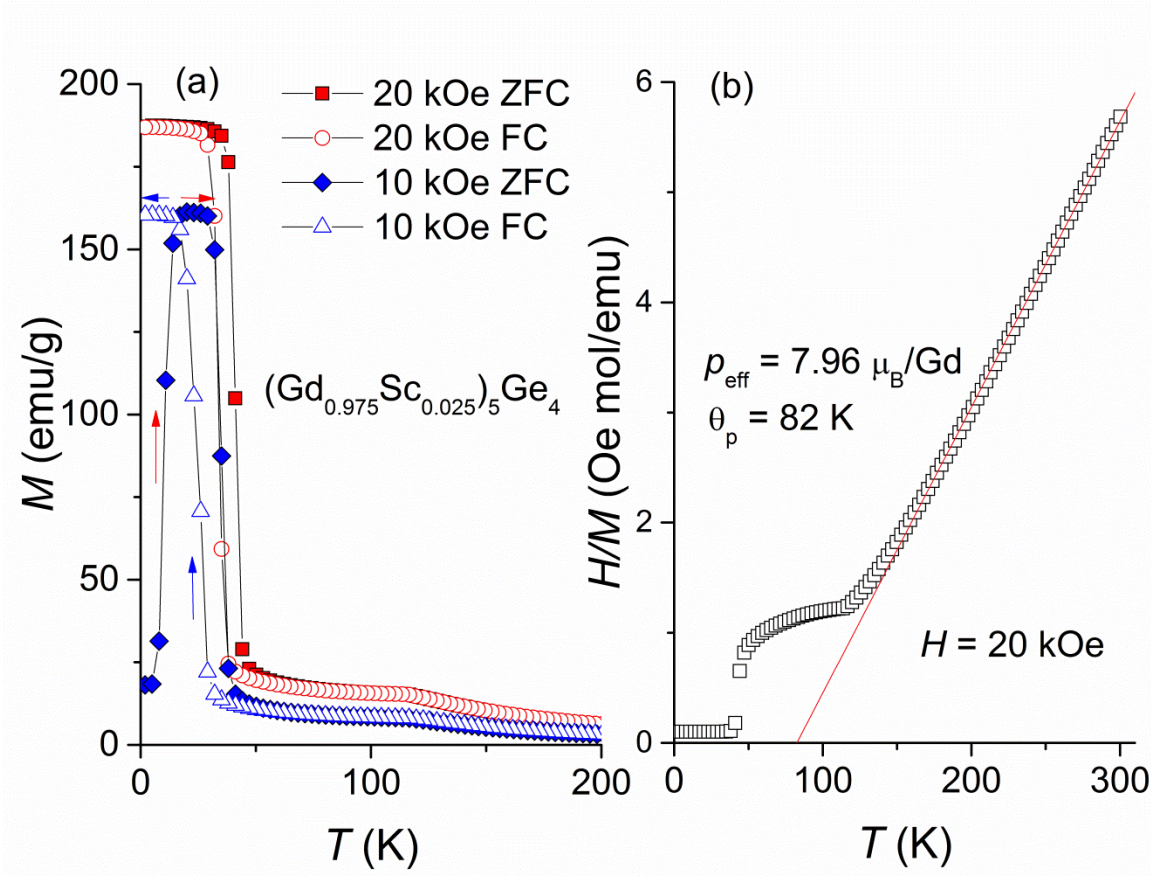

Figure 2. (Color online) (a) Temperature dependencies of the dc magnetization of $(Gd_{0.975}Sc_{0.025})_5Ge_4$ measured in 10 and 20 kOe applied magnetic fields. (b) The temperature dependence of the inverse susceptibility (H/M) vs. T for 20 kOe applied field. The red solid line represents the Curie-Weiss fit to the experimental data.

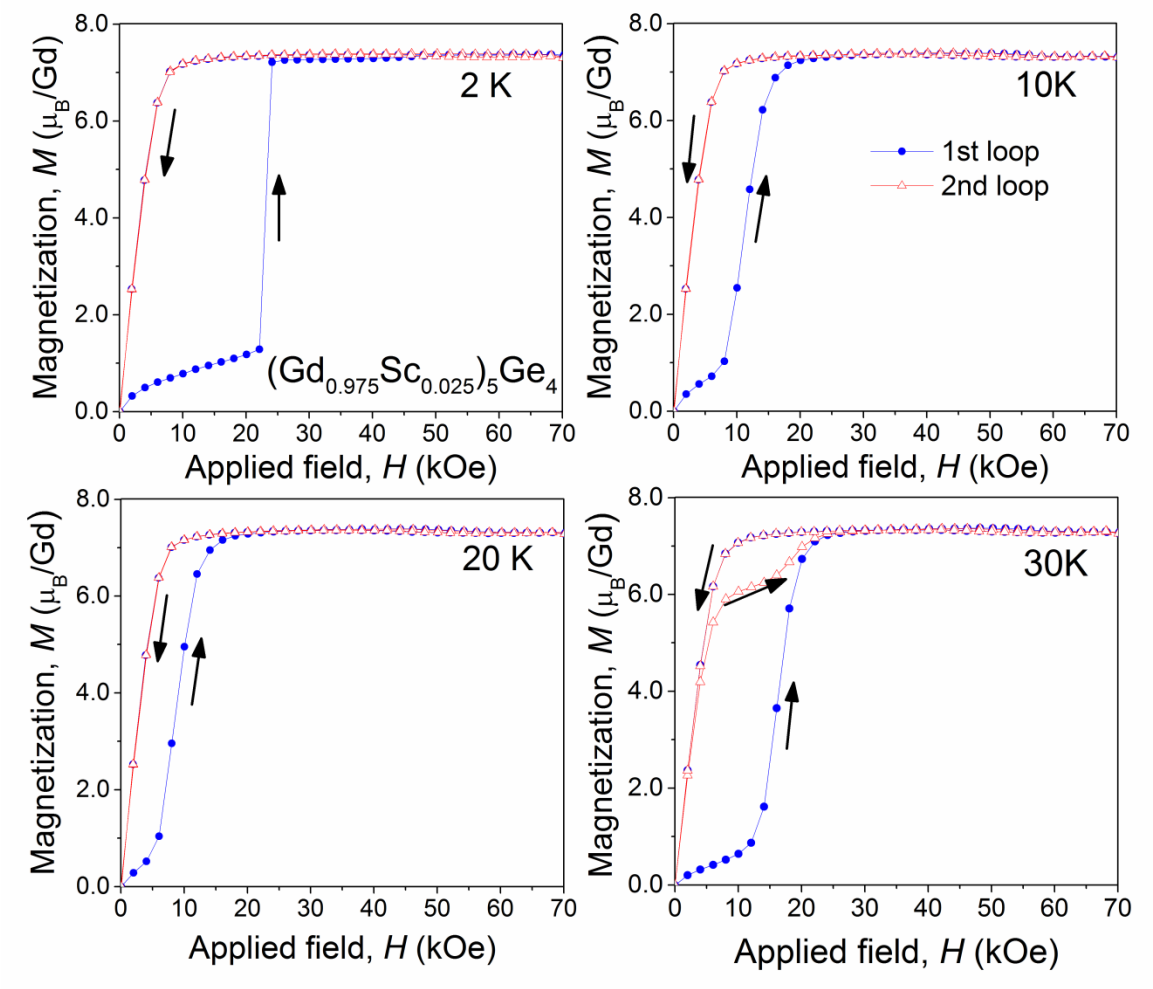

Figure 3. (Color online) The isothermal magnetization of $(Gd_{0.975}Sc_{0.025})_5Ge_4$ at 2, 10, 20, and 30 K. Solid blue circles indicate the first magnetization/demagnetization cycle and the open red triangles indicate the second magnetization/demagnetization cycle.

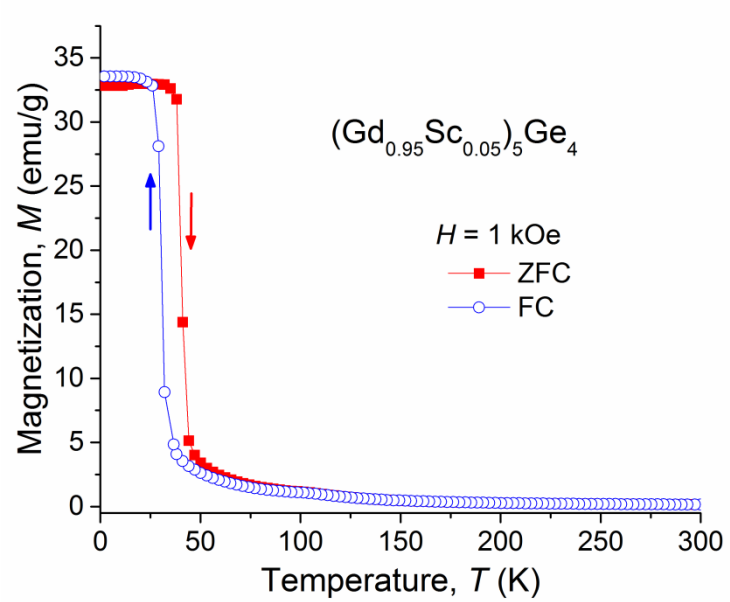

Figure 4. (Color online) Temperature dependencies of the dc magnetization of $(Gd_{0.95}Sc_{0.05})_5Ge_4$ measured in a 1 kOe applied magnetic field with ZFC and FC protocols.

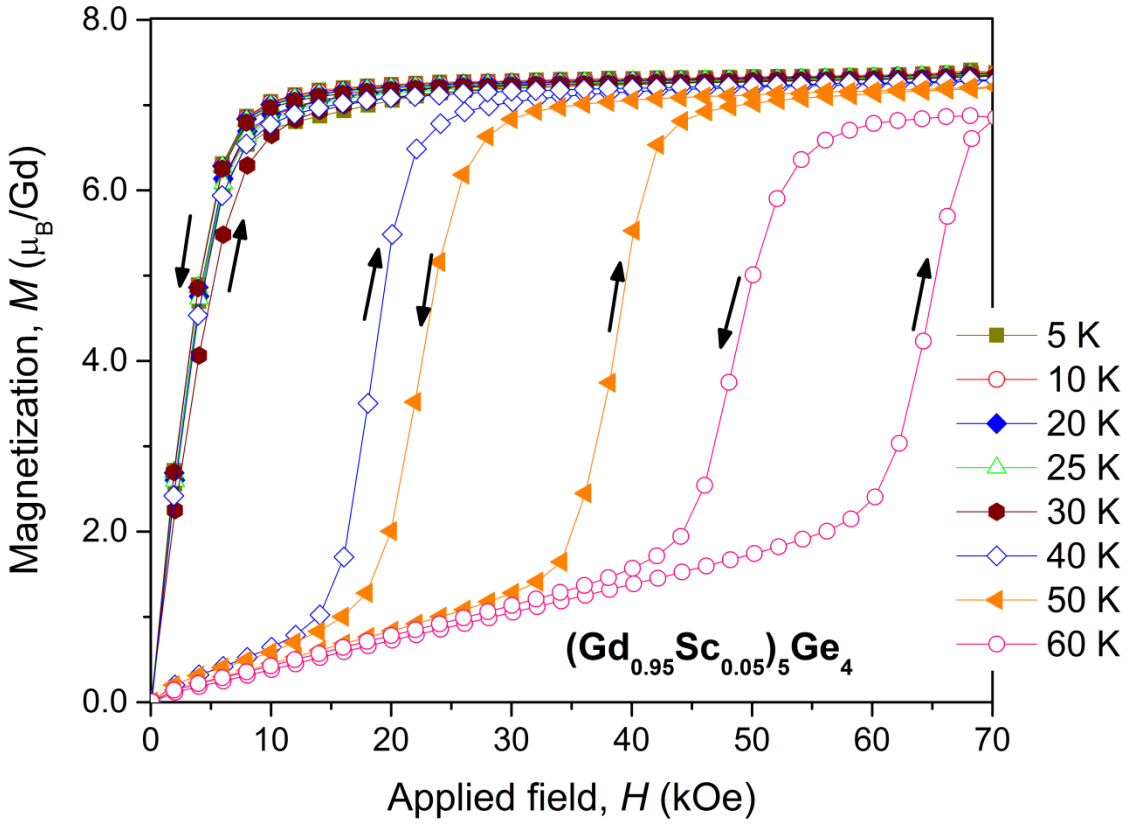

Figure 5. (Color online) The isothermal magnetization of $(Gd_{0.95}Sc_{0.05})_5Ge_4$ measured in the range of temperatures from 5 to 60 K.

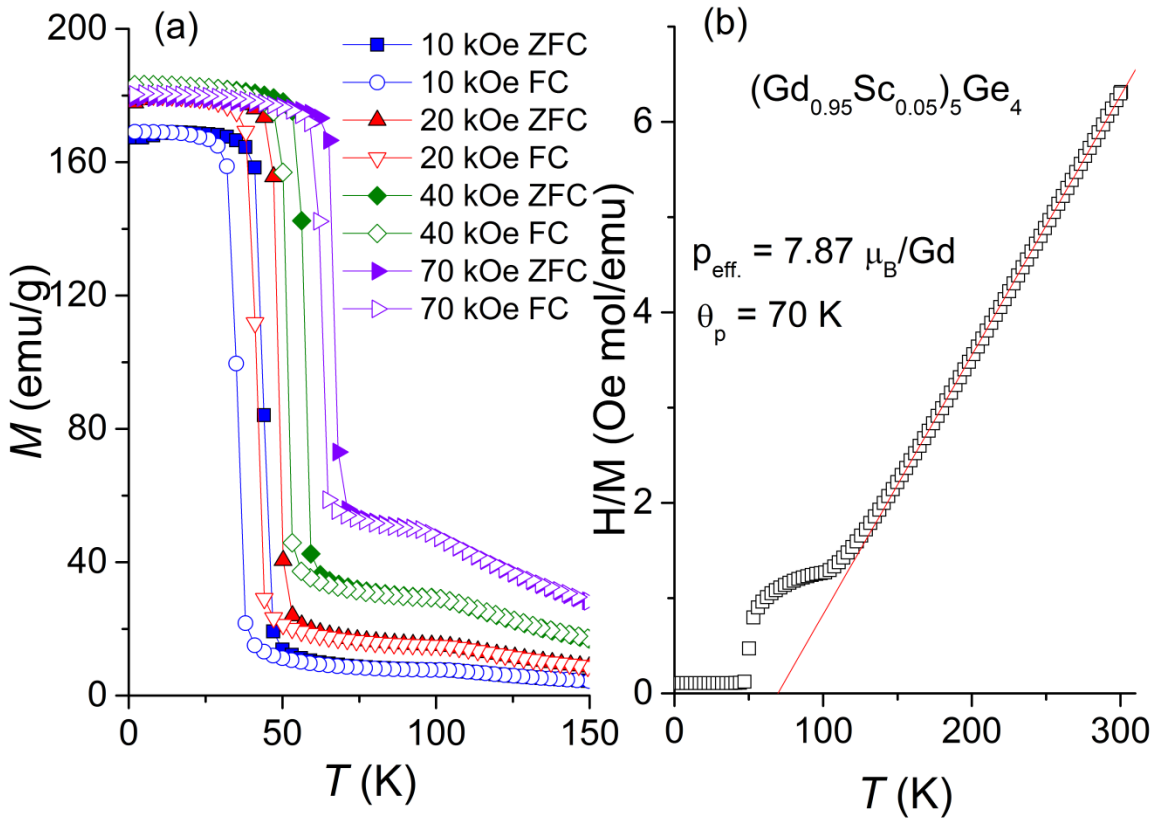

Figure 6. (Color online) (a) Temperature dependencies of the dc magnetization of $(Gd_{0.95}Sc_{0.05})_5Ge_4$ measured in 10, 20, 40, and 70 kOe applied magnetic fields with ZFC and FC protocols. (b) The temperature dependence of the inverse susceptibility (H/M) vs. T obtained under the 20 kOe applied field. The red solid line represents the Curie-Weiss fit to the experimental data.

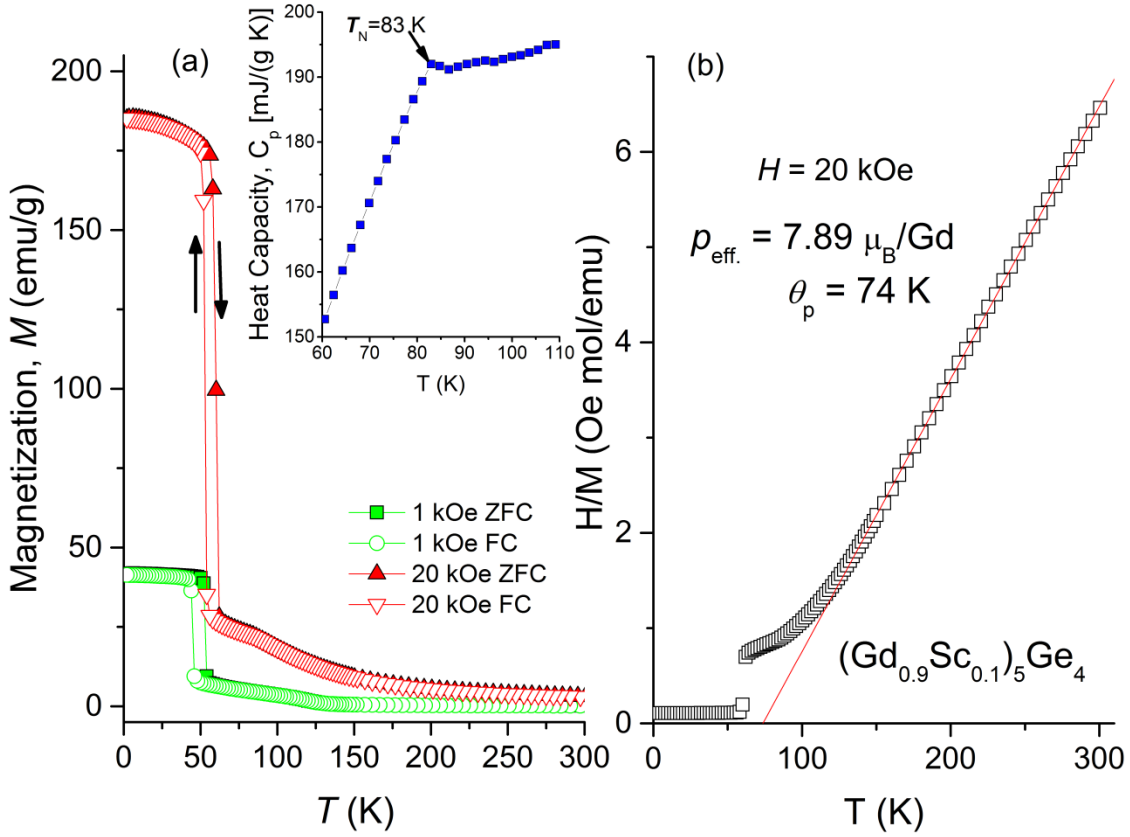

Figure 7. (Color online) (a) Temperature dependencies of the dc magnetization of $(Gd_{0.9}Sc_{0.1})_5Ge_4$ measured in 1 kOe and 20 kOe applied magnetic field with ZFC and FC protocols. The inset highlight the AFM-PM transition observed in zero field heat capacity data between 60 and 110 K. (b) The temperature dependence of the inverse susceptibility (H/M) vs. T obtained under the 20 kOe applied field. The red solid line represents the Curie-Weiss fit to the experimental data.

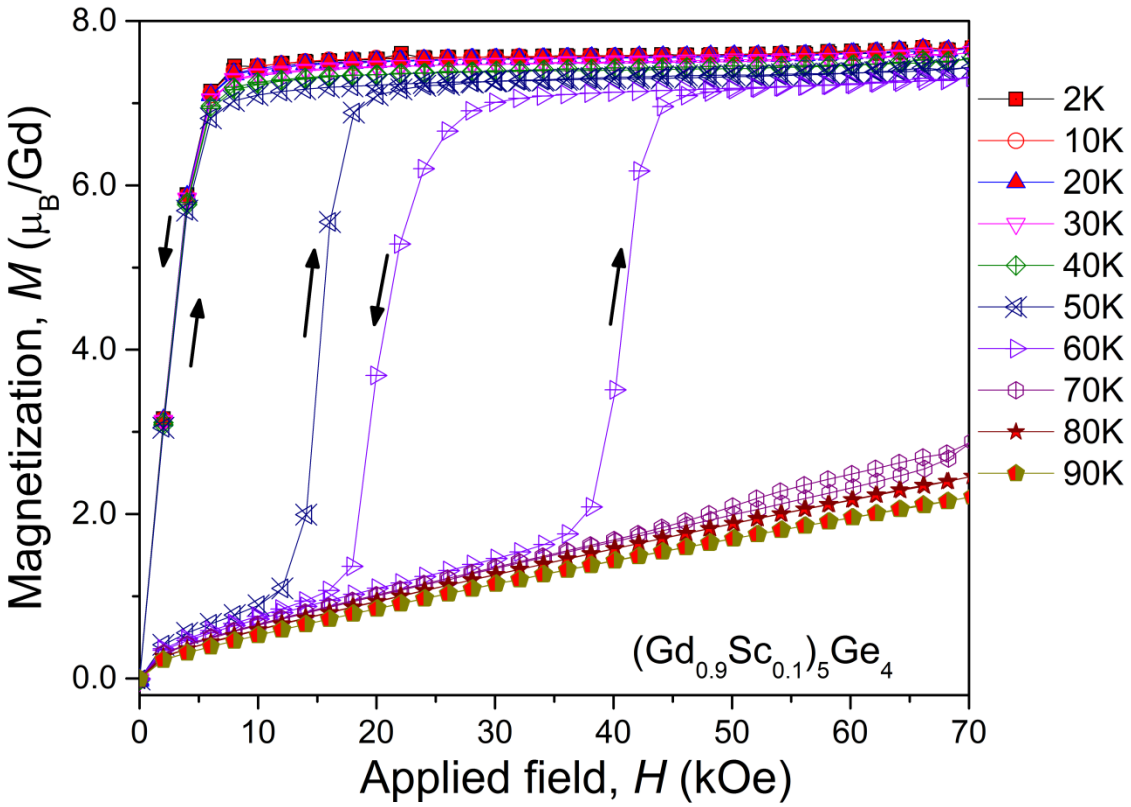

Figure 8. (Color online) The isothermal magnetization of $(Gd_{0.9}Sc_{0.1})_5Ge_4$ measured in the range of temperatures from 2 to 90 K.

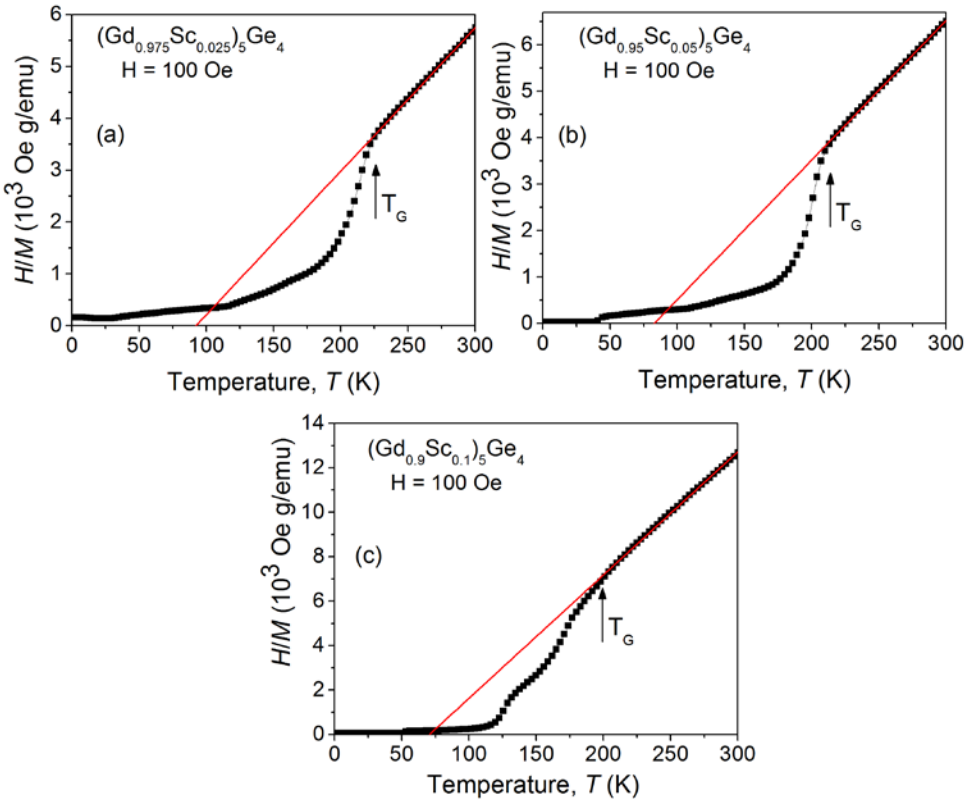

Figure 9. (Color online) The inverse dc magnetic susceptibility (H/M) of $(Gd_{1-x}Sc_x)_5Ge_4$ (x = 0.025 (a), 0.05 (b), and 0.1 (c)) measured in a 100 Oe dc magnetic field.

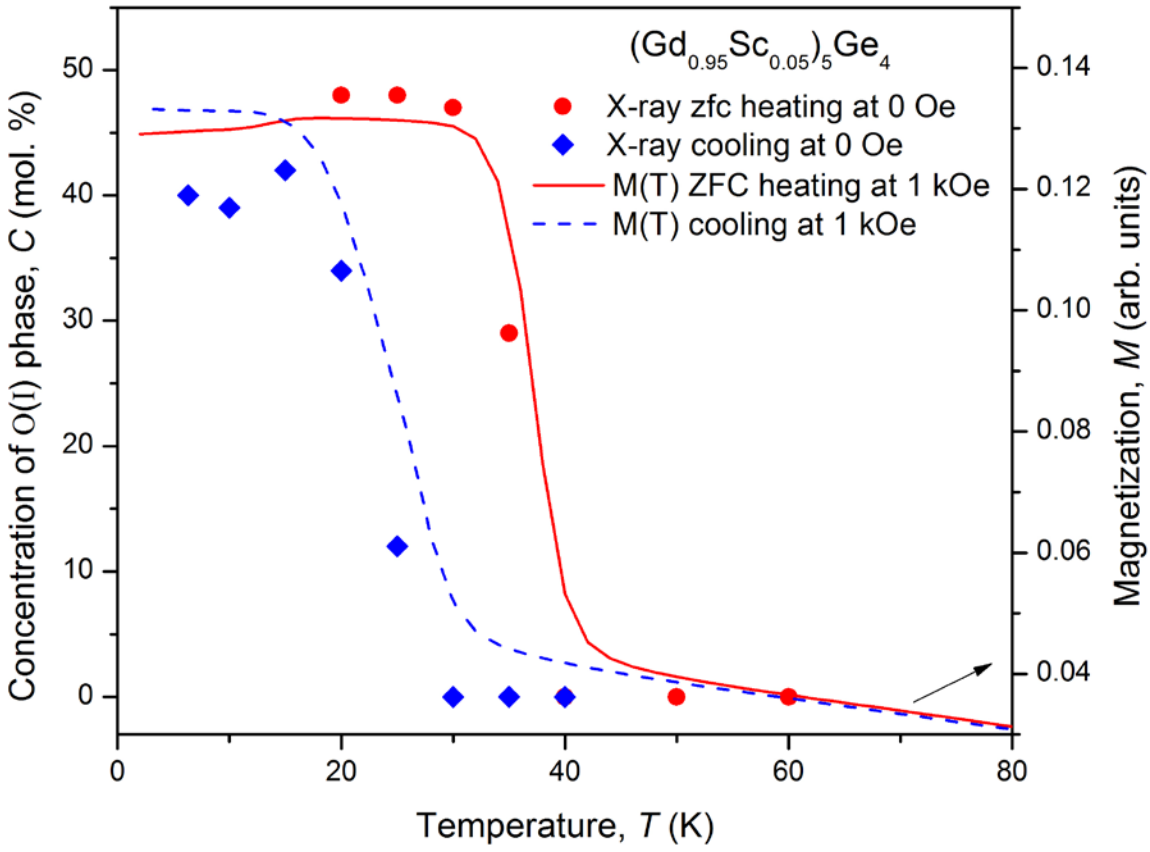

Figure 10. (Color online) Concentration of the O(I)-$(Gd_{0.95}Sc_{0.05})_5Ge_4$ phase as a function of temperature (symbols, left hand scale) determined from the powder X-ray diffraction experiment during heating and cooling in zero magnetic field and the dc magnetization of $(Gd_{0.95}Sc_{0.05})_5Ge_4$ powder sample measured in 1 kOe magnetic field (thick lines, right hand scale) during heating and cooling. Arbitrary units are used because the powder was mixed with varnish and its exact mass was unknown.

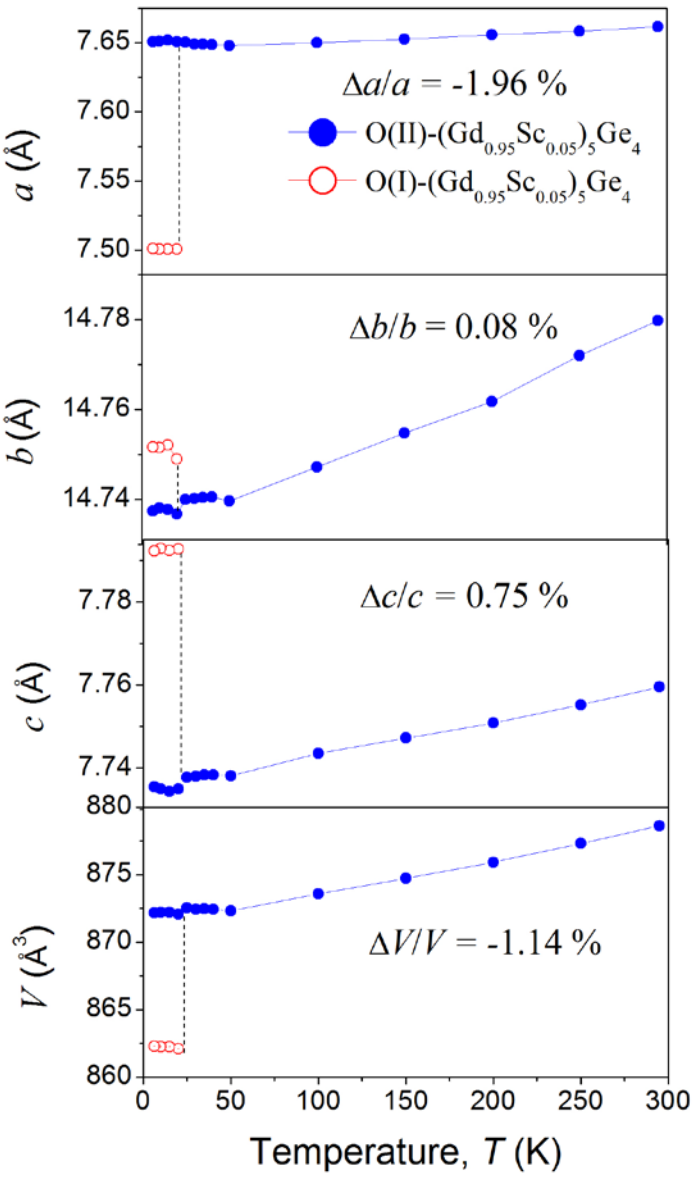

Figure 11. (Color online) Temperature dependencies of the lattice parameters and the unit-cell volume of $(Gd_{0.95}Sc_{0.05})_5Ge_4$ determined from 6.3 to 300 K in a zero magnetic field on cooling. The solid circles indicate lattice constants of the high-temperature O(II) structure, which is present down to the lowest temperature of the measurement. The open circles indicate lattice constants of the high-temperature O(I) structure.

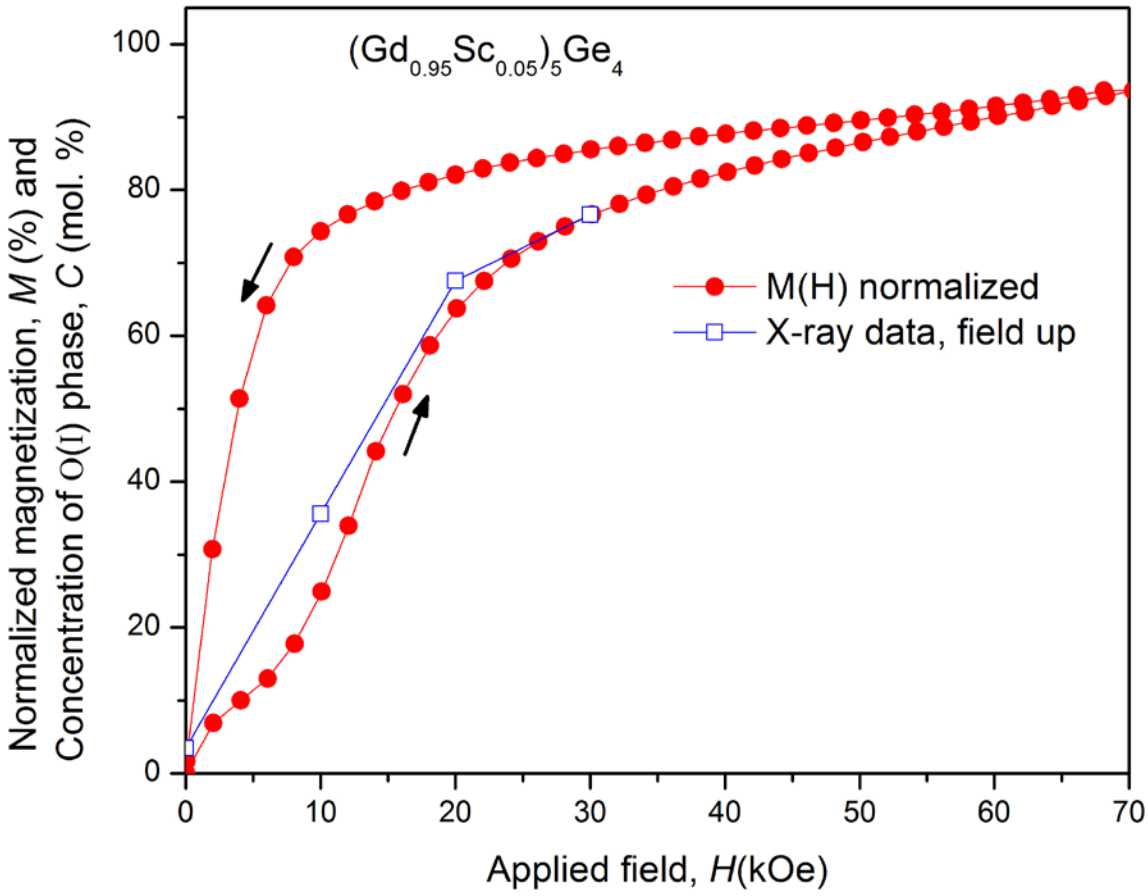

Figure 12. (Color online) The comparison of the magnetic field dependence of the O(I) phase concentration determined using the powder X-ray diffraction (open squares) with the normalized magnetization of $(Gd_{0.95}Sc_{0.05})_5Ge_4$ (solid circles) at 30 K.

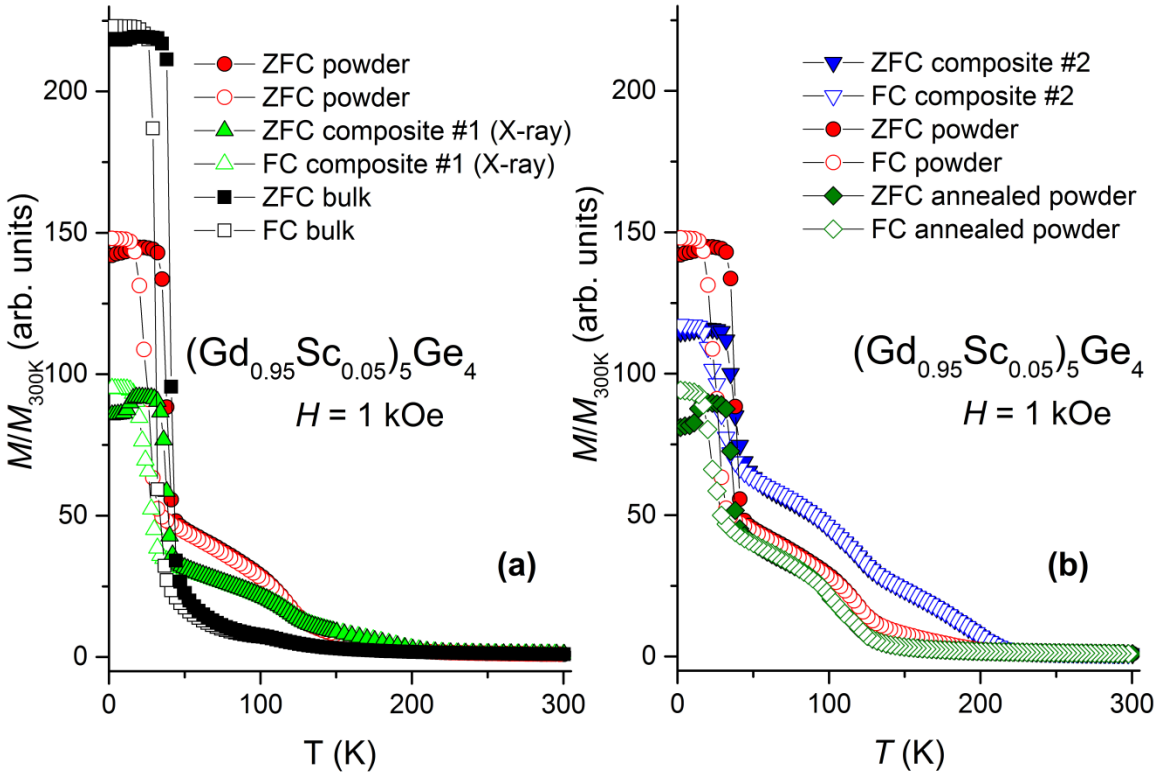

Figure 13. (Color online) (a) Temperature dependency of magnetization of the $(Gd_{0.95}Sc_{0.05})_5Ge_4$ bulk, powder, and composite #1 (X-ray sample) materials measured from 2 to 300 K in magnetic field of 1 kOe. (b) Temperature dependency of magnetization of the $(Gd_{0.95}Sc_{0.05})_5Ge_4$ as-milled powder, annealed (500 °C/20 min) powder and composite #2 measured from 2 to 300 K in magnetic field of 1 kOe.

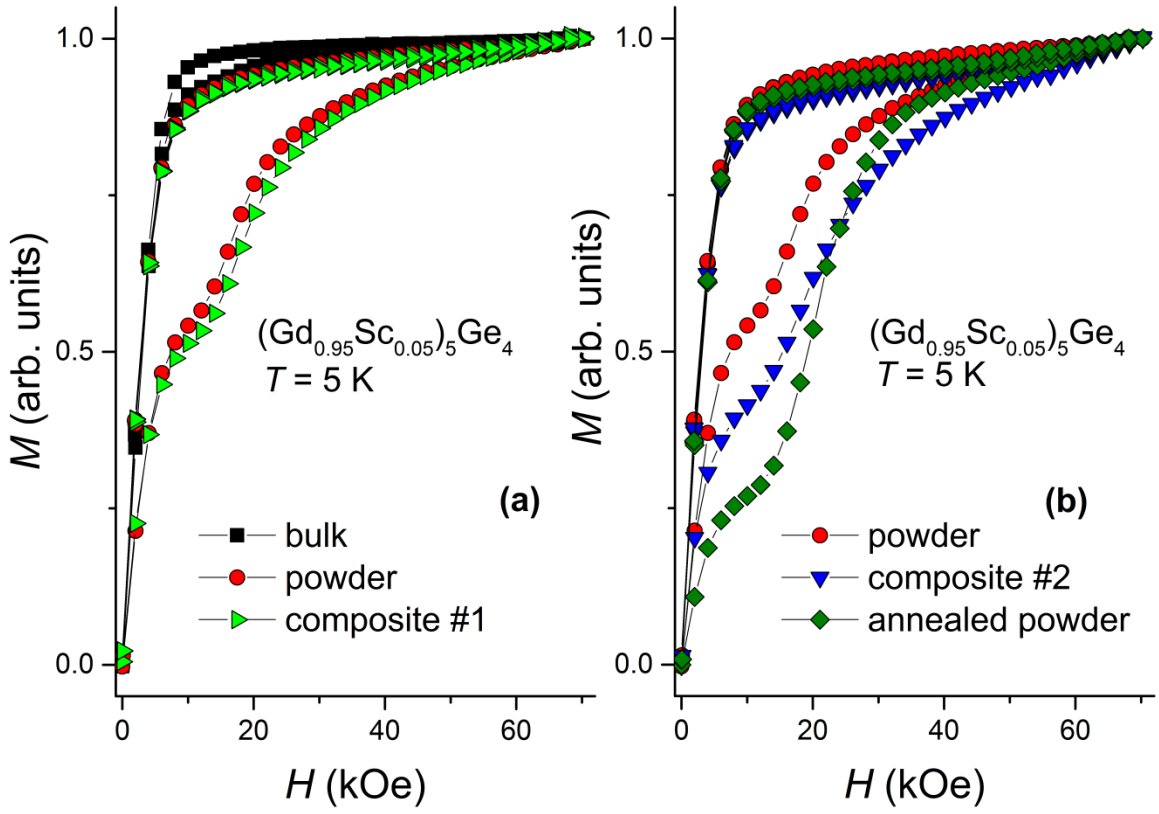

Figure 14. (Color online) (a) Isothermal dc magnetization of the bulk, powder, and composite #1 samples of $(Gd_{0.95}Sc_{0.05})_5Ge_4$ at 5 K. (b) Isothermal dc magnetization of the as-milled powder, annealed powder, and composite #2 sample of $(Gd_{0.95}Sc_{0.05})_5Ge_4$ at 5 K.